

## Epoxy/Copper Oxide Composite Coating for Marine Application

Kautsar Binti Tabri<sup>a</sup>, Nor Yuliana Yuhana<sup>ab\*</sup>, Jafreena Adira Jaafar<sup>b</sup>, Ahmad Faiz Al Shafie<sup>c</sup> & Mohammad Aslamilie Mohd Suhil<sup>c</sup>

<sup>a</sup>Department of Chemical & Process Engineering

<sup>b</sup>Research Centre for Sustainable Process Technology (CESPRO),  
Faculty of Engineering & Built Environment, Universiti Kebangsaan Malaysia, Malaysia

<sup>c</sup>Bina Integrated Industries Sdn. Bhd.,  
No. 10 Jalang/7, Taman IKS, Seksyen 9, 43650 Bandar Baru Bangi, Selangor, Malaysia.

\*Corresponding author: yuliana@ukm.edu.my

Received 07 June 2018, Received in revised form 25 July 2020  
Accepted 09 November 2020, Available online 28 February 2021

### ABSTRACT

*This research investigated the usage of cuprous oxide powder as filler for epoxy in marine coating industries. The basic formulation consist of cuprous oxide powder, epoxy pre-polymer, and the curing agent. The main manipulation variable in this research is the quantity of cuprous oxide added into the epoxy resin, which varies from 2, 5, 7, 9, and 11 per hundred gram of epoxy resin (phr). Polyether (amine) was used as the curing agent at equivalent molar ratio. Mechanical stirring was used to achieve dispersion. The samples were cured at room temperature for one week before characterization. Differential scanning calorimetry (DSC), scanning electron microscopy (SEM), infrared spectroscopy (FTIR), X-ray diffraction (XRD), drop shape, water and brine absorption, hardness, and abrasion analysis were used. Drop shape analysis exhibited the hydrophobicity of the surfaces. According to water and brine absorption test that was carried out, it is found that the unmodified epoxy sample has the lowest absorption of water and brine. The composite coating, which underwent abrasion test, exhibited increasing hydrophobicity of the surface directed on the electrical wave generator in 5 days.*

*Keywords: Cuprous oxide, Epoxy resin, Hydrophobicity, Curing*

### INTRODUCTION

Coating is a layer that acts as a barrier from corrosion to occur when applied on an object (Anon. 2017). There are three types of coatings in industry, which mainly are trade sale paint, industrial coatings (including marine coatings), and inorganic coatings). Marine coating technology has existed for the past 2000 years, and different parts of a ship require different type of coatings as their environments distinct (Ray et al. 2017). One of marine coating types is anti-fouling category. According to Dafforn et al. (2011), generally, there are four types of anti-fouling systems, which are soluble matrix, contact leaching, self-polishing copolymer, and foul release. The mechanisms of marine coatings can be illustrated in Figure 1.

Figure 1 (a) shows the soluble matrix coating system, which the copper particle and the biocide stimulator will spread through the coating binder system into the seawater. Next, Figure 1(b) is the contact leaching system where the binder will not solubilize but only the biocide and its booster will leach out into the system. Figure 1(c) is the self-polishing system. What makes self-polishing system differs from soluble matrix is that the biocide and booster of the soluble matrix system will be running out first then only its matrix or binder system, whereby both the biocide and the matrix of the self-polishing system will run out at exactly

the same time. Lastly, foul release system is really different from the other three systems in which this system does not involve any usage of biocide or causing any leaching into the seawater. It just imitates the water movement using silicon with low energy surface, disabling the microorganisms to stick on its surface.

Basically, coating is made up of four substances called binder, pigment, additive and solvent. Binder acts as the medium of binding all the particle inside the coating that makes up the physical and chemical traits of the coating. Resin epoxy is one of the most important classes of thermoset due to its excellent physical and chemical properties, such as absence of byproduct or volatiles during curing process, curing at big range of temperatures, and has controlled crosslinking. Epoxy resin also has been used widely since the 20<sup>th</sup> century with its aliphatic amine curing agent in coating industries and application on structures due to its outstanding thermal, mechanical, and electrical properties (Mirmohseni et al. 2010; Sorolodoni et al. 2017; Paik Sung et al. 2005; Yebra et al. 2006; Adeleye et al. 2016).

Talking about pigment, the main characteristic that is fundamental in choosing the suitable pigment is its size, structure, and the shape of particle (Yebra et al. 2009). Cuprous oxide is the main pigment used for massive production in industries (El Saeed et al. 2016). Copper technology is being widely used due to its ability to act

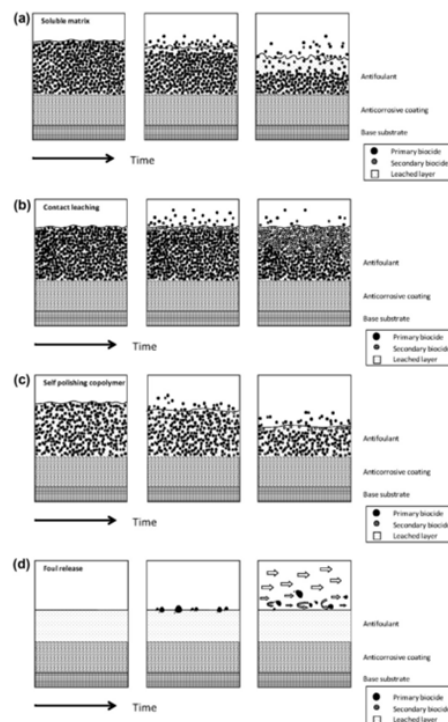


FIGURE 1. Types of anti-fouling systems (Marine Pollution Bulletin, 2011)



FIGURE 2. FTIR machine (Nicolet 6700 machine)

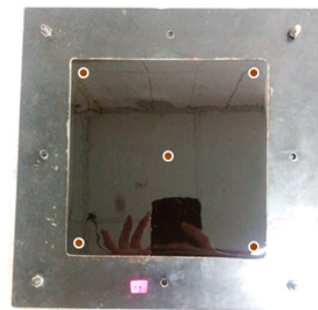


FIGURE 3. Points indenter exerted

as marine bio-fouling inhibitor and self-polishing trait. According to a study by California university student, the release of copper is influenced by some factors, such as the salinity of water, type of coated surface, and drying time. It is found that a coated wood had a higher rate of biocide release rather than a coated aluminum surface (Adeleye et al. 2016). It is said that zinc release is slower than copper release when the sunlight is absent (Holmes et al. 2009).

Solution or curing agent could be either chemical solution or water. Coating that use water as soluble medium will face several problems, such as taking time to dry and absorbing water. That is why coating system that uses chemical solution has its own benefits as compared to just plain water (Yebra et al. 2009). Additives can be multi-functional in assisting towards better coating system as they can be anti-corrosive, degassing, non-thinning, dispersant assist, etc. (Lambourne et al. 1999).

Marine bio-fouling is a natural phenomenon that can cause serious problems economically. It is triggered when

a layer community of microorganisms or biofilm formation formed on the substrate surface area, causing the bigger parasitic livings, such as barnacles, to easily attached on the surfaces that are layered with biofilm (Yebra et al. 2006).

## METHODOLOGY

### SAMPLE PREPARATION

100 gram of epoxy resin was heated until 55 - 60°C and then, certain weight of cuprous oxide were mixed by using mechanical stirring for 1 hour with the speed of 50 rpm. Polyether amine at equimolar ratio was added and the mixture was stirred for 10 minutes. The mixture was then poured into a 100 mm x 100 mm x 5 mm mold and was let to be cured for one week at room temperature. Then, the sample preparation was repeated with 0 gram, 2 gram, 5 gram, 7 gram, 9 gram, and 11 gram of cuprous oxide. The

TABLE 1. DSC analysis technique

Phase	Temperature range (°C)	Heating or cooling rate
Phase 1	25 until 170	10°C per minute
Phase 2	170	170°C per two minutes
Phase 3	170 to -20	20°C per minute
Phase 4	-20 to 170	10°C per minute

cured samples were then sent to several analysis for physical and chemical traits characterization.

#### FTIR ANALYSIS

FTIR (Fourier Transform Infrared Spectroscopy) is a technique commonly used to control the quality of material produced when an industrial evaluation is conducted. This technique is the first step taken to analyze the components contained in a sample. The changes in FTIR curve produced signify the change in the composition or the impurities contained. When epoxy resin was cured with an aliphatic amine liquid, the present functional group in epoxy resin will be different when the coating underwent curing process.

#### DSC ANALYSIS

Differential scanning calorimeter (DSC) analysis using Mettler Toledo DSC 822e was used to ensure that the samples are fully cured and observing the glass transition temperature of the samples. The DSC program is as in Table 1.

#### SEM ANALYSIS

The scanning of electron microscopy (SEM) was performed using ZEISS SIGMA VP Field Emission Scanning Electron Microscopes (FE-SEM). SEM analysis is a useful tool for specimen surface study. A thin film of platinum was added to the coating before being scanned with a high – energy electron beam across the surfaces. Then, the samples were examined at magnification with the scale of 10  $\mu\text{m}$ , 2  $\mu\text{m}$ , 1  $\mu\text{m}$ , and 200 nm.

#### XRD ANALYSIS

XRD analysis was performed using Bruker X-Ray Diffractometer model D8 ADVANCE. This investigation activity was carried out within 2 theta ranges from 5° until 80° and scanning rate of 0.025 per minute.

#### DROP SHAPE ANALYSIS

Drop shape analysis (DSA) was performed using Drop Shape Analyzer-DSA100 and the contact angle obtained will reflect either the surface is hydrophobic or hydrophilic. A surface is considered hydrophobic when the contact angle exceeds 90°.

#### SIZE PARTICLE ANALYSIS

ZETASIZER analysis was conducted using Malvern Mastersizer 2000 particle size analyzer for cuprous oxide powder.

#### ROCKWELL HARDNESS TEST

Samples sized 100 mm x 100 mm x 5 mm were tested with Digital Rockwell Hardness Tester – Rocky D using a HRL indenter. The indenter exerts force on 5 points on the sample as in FIGURE 3.

#### WATER AND BRINE ABSORPTION

Samples were cut into 100 mm x 50 mm x 5 mm size and each of the samples was weighted before inserted into a three-liter container. Then, 2 liter of distilled water was added into the respective containers and the samples were let to submerge for 7 days. The samples were dried and weighted for every 24 hours to know the rate of water adsorption. For brine absorption, the method used was just the same as water absorption, except for the medium of submerging. The concentration of salt in the brine was 35 g/mL.

#### ABRASION TEST

Resistance to abrasion of the coating was tested with a physical simulation using a 13 liter container, an electric wave generator with 3000 L/h fluid flow rate, polystyrene balls with an average diameter of 7 mm, resembling the diatomaceous earth, brine, fluorescence lamp, and flexible coating holder. The test was set up as in FIGURE 4.

Then, the wave from the electric generator was let to hit the surface of coating continuously for 5 days. Contact angle of the surface was measured before and after the test to acknowledge the changes in hydrophobicity.

#### RESULTS AND DISCUSSIONS

##### FTIR ANALYSIS

FTIR wavenumber pattern of each sample was very similar to each other. Only some differences could be found within certain wavenumber range. FIGURE 5 exhibits the FTIR analysis graph for epoxy resin coating containing 2 phr, 5 phr, 7 phr, 9 phr, and 11 phr.

The graph shows that there is a minor difference in bands, ranges from  $2325\text{ cm}^{-1}$  to  $1949\text{ cm}^{-1}$ . For samples Epoxy/2g  $\text{Cu}_2\text{O}$  and Epoxy/5g  $\text{Cu}_2\text{O}$ , there is only one peak exists in the range of  $2120.9\text{ cm}^{-1}$ . Whereas for sample Epoxy/7g  $\text{Cu}_2\text{O}$ , there are two peaks exist within the same wavenumber range. But, for sample Epoxy/9g  $\text{Cu}_2\text{O}$  and Epoxy/11g  $\text{Cu}_2\text{O}$ , three peaks are observed. According to Anon (2015), any changes in the absorption band pattern indicate changes in the composition of the materials in the sample. It can therefore be concluded that there is an increase in peak in the absorption band for the range  $2325\text{ cm}^{-1}$  to  $1949\text{ cm}^{-1}$  when the weight of copper oxide increases, indirectly indicating changes in composition in the sample.

#### DSC ANALYSIS

Based on results obtained, during the first heating, the endothermic peaks were observed in all samples, indicating the possibility of melting process occurred for polyetheramine or some unknown materials. The presence of exothermic peak during heating shows that the materials are fully reacted. Glass transition differs for every sample as in Table 2.

#### SEM ANALYSIS

Morphology study of cuprous oxide coating was carried out to find out the dispersion of cuprous oxide on the surface. Yu et al. (2009) observed that copper oxide creates a pore network on the surface of coating.

Figure 7 shows the SEM analysis diagram for the Epoxy/5g  $\text{Cu}_2\text{O}$  sample at 1000 times magnification. The well-arranged copper oxide particle on the coating surface was interesting to be further studied. As the amount of filler increased, the more compact was the arrangement of filler on the surface. Figure 8 shows the SEM analysis diagram for the Epoxy/11g  $\text{Cu}_2\text{O}$ .

At 30,000 times magnification, the irregular shape of copper oxide was observed in which cubic shape seems to be dominant for Epoxy/5g  $\text{Cu}_2\text{O}$  as shown in Figure 9. However, for sample Epoxy/11g  $\text{Cu}_2\text{O}$ , it was observed that there is agglomeration of spherical fine particles as in Figure 10.

It can be seen in Figure 9 and Figure 10 that there are significant differences in the size and shape of copper oxide particles. Cuprous oxide in Figure 9 had various uneven particle shapes of cube and sphere.

While in Figure 10, the cuprous oxide deposits in small craters in a particular point area are embedded on the surface. Among the factors that affected the particle size of cuprous oxide were believed to be due to saturation of cuprous oxide powder in the coating. When the quantity of cuprous oxide powder in the coating increases, this will cause filler particles to collide with each other, colliding with the wall of stirring and stirring blades. Hence, due to continuous violation momentum for one hour at a speed of 50 rpm, the cuprous oxide particles break down to smaller sizes.

#### XRD ANALYSIS

Crystallographic of certain samples were studied to acknowledge the degree of particle structuring. If compared, XRD analysis graph of Epoxy/5 g  $\text{Cu}_2\text{O}$  sample and Epoxy/11 g  $\text{Cu}_2\text{O}$  sample, there are peaks for both graphs between  $2\theta = 8^\circ$  and  $2\theta = 24^\circ$ .

The peaks are clearly observed at  $2\theta = 8^\circ$ ,  $14^\circ$ , and  $22^\circ$  for sample of the Epoxy/5g  $\text{Cu}_2\text{O}$ . However, Epoxy/11g  $\text{Cu}_2\text{O}$  only shows 2 peaks, which indicate that varying the weight of  $\text{Cu}_2\text{O}$  can alter the morphology and crystallinity of composite samples as shown in Figure 12.

#### DROP SHAPE ANALYSIS

Table 3 shows the results of the contact angle analysis obtained from the analysis laboratory. A total of 99 computations have been taken and quantified using the appropriate software to measure the water droplet contact angle on the surface of samples.

The highest contact angle value is  $94.2^\circ$  belonged to Epoxy/2g  $\text{Cu}_2\text{O}$  sample, while the lowest contact angle value is  $67.4^\circ$  belonged to the unmodified epoxy sample. These results signify that the optimum number of filler additions into resin epoxy is 2 gram. Based on the data contained in Table 2, the addition of cuprous oxide powder could increase the contact angle of a coating. However, the value of the contact angle decreased after the quantity of filler exceeded 2 g indicating the maximum.

#### PARTICLE SIZE ANALYZER

Table 4 represents the variety of size ranges in powder of cuprous oxide. The inconsistent results from several tests could be due to the large size range of cuprous oxide particle.

#### ROCKWELL HARDNESS TEST

It was found that Epoxy/11g  $\text{Cu}_2\text{O}$  sample had the highest hardness value at 89.1 HRL whereby the lowest hardness was Epoxy/7g  $\text{Cu}_2\text{O}$  at 85.14 HRL as in Figure 13.

This might be due to the inconsistency of cuprous oxide dispersity on coatings' surfaces as observed in SEM analysis diagram and non-discrete particle size of filler. It is believed that the hardness of the coating synthesized was higher at the spot rich in cuprous oxide as compared to the spot with less cuprous oxide.

#### WATER AND BRINE ABSORPTION

This test was conducted for 7 continuous days for each sample with different PHR. The water absorption rate was measured within 24 hours from time to time until a week was completed. The results of water absorption can be observed in Figure 14.

Based on the observations made, the results exhibit that the unmodified sample had the lowest water absorption, whereas Epoxy/5g  $\text{Cu}_2\text{O}$  had the highest water absorption.

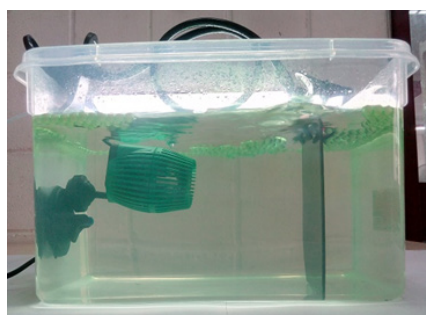


FIGURE 4. Abrasion test set up

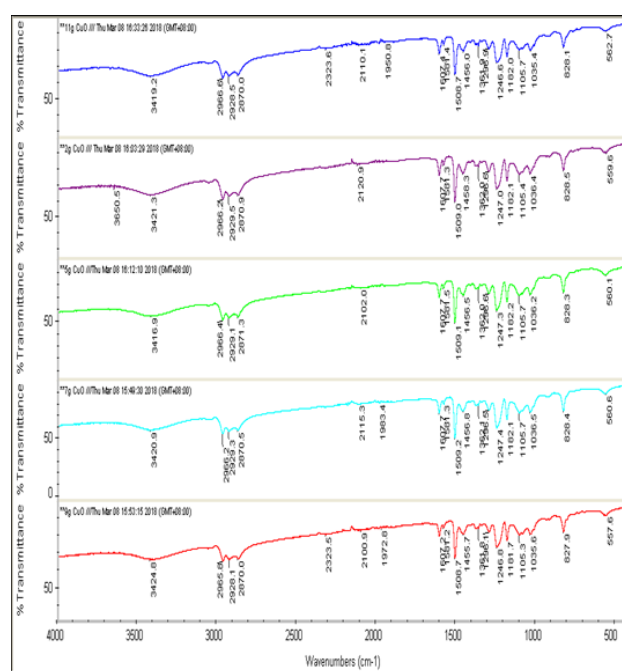


FIGURE 5. Combined FTIR analysis graph for all samples

TABLE 2. Glass transition temperature of samples

Sample	Glass transition temperature onset (°C)	Glass transition temperature midpoint ISO (°C)
Epoxy/2g Cu <sub>2</sub> O	83.02	86.79
Epoxy/5g Cu <sub>2</sub> O	80.90	84.41
Epoxy/7g Cu <sub>2</sub> O	76.55	82.40
Epoxy/9g Cu <sub>2</sub> O	82.75	86.57
Epoxy/11g Cu <sub>2</sub> O	81.04	85.63

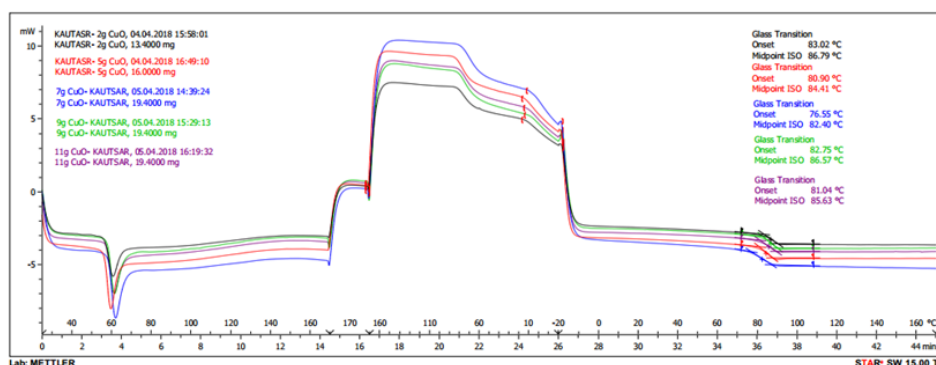


FIGURE 6. Combined DSC analysis graph for all samples



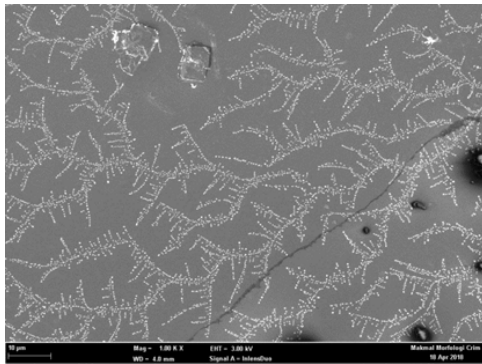


FIGURE 7. SEM result for Epoxy/5g Cu<sub>2</sub>O

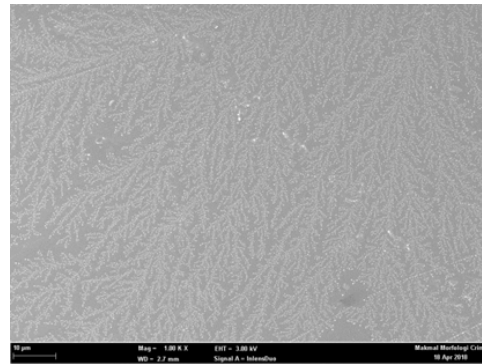


FIGURE 8. SEM result for Epoxy/11g Cu<sub>2</sub>O

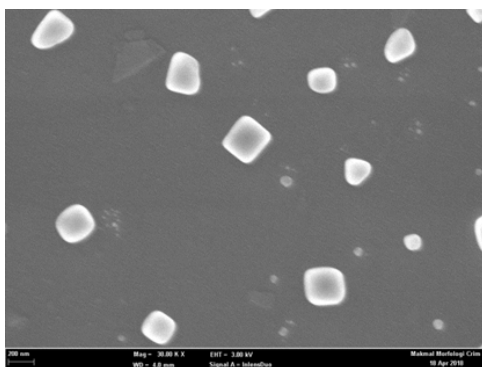


FIGURE 9. SEM result for Epoxy/5g Cu<sub>2</sub>O

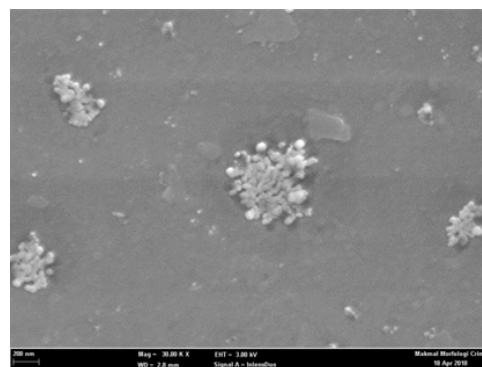


FIGURE 10. SEM result for Epoxy/11g Cu<sub>2</sub>O

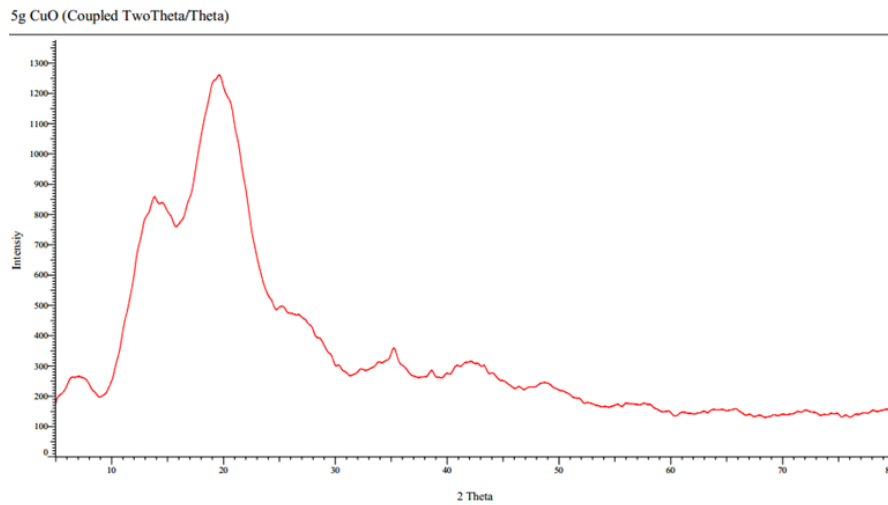


FIGURE 11. XRD analysis graph for Epoxy/5 g Cu<sub>2</sub>O sample

When synthesizing Epoxy/5g Cu<sub>2</sub>O, its surface was found to be sticky, indicating a tendency of uncured coating samples that were produced, hence affected the properties of composite.

For brine absorption, the unmodified epoxy still gave the lowest absorption percentage, but the highest brine absorption was Epoxy/7g Cu<sub>2</sub>O as in Figure 15. This phenomenon happened may due to the particle structuring in filler particle. Floatable filler particle provides better brine and water absorption in terms of improving its permeability to any type of medium transmittance passby.

ABRASION TEST

The properties of the coating were characterized by contact angle value of the preliminary and post abrasion test. Table 5 below shows the overall result of this test.

Based on Table 5, it is found that the contact angle value of both samples ascending after the abrasion test was carried out. These results acted as evidence that the resulting coating is self-polished. However, the unmodified samples have higher contact angle value than Epoxy/2g Cu<sub>2</sub>O. Contact angle value is closely

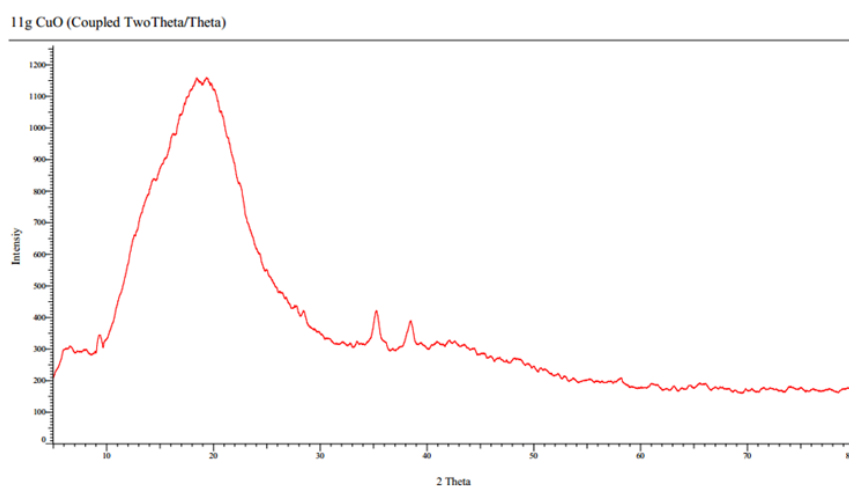
FIGURE 12. XRD analysis graph for Epoxy/11g Cu<sub>2</sub>O sample

TABLE 3. Drop shape analysis results

Sample	Contact angle (°)
Epoxy	67.4 ± 0.07
Epoxy/2g Cu <sub>2</sub> O	94.2 ± 2.11
Epoxy/5g Cu <sub>2</sub> O	76.1 ± 0.50
Epoxy/7g Cu <sub>2</sub> O	85.1 ± 0.98
Epoxy/9g Cu <sub>2</sub> O	79.4 ± 0.34
Epoxy/11g Cu <sub>2</sub> O	78.2 ± 6.60

TABLE 4. Particle size of cuprous oxide powder

Sample	Average diameter (nm)	Size range (nm)
Sample 1	352.0	200 – 850
Sample 2	362.5	60 – 6500
Sample 3	342.6	55 6500

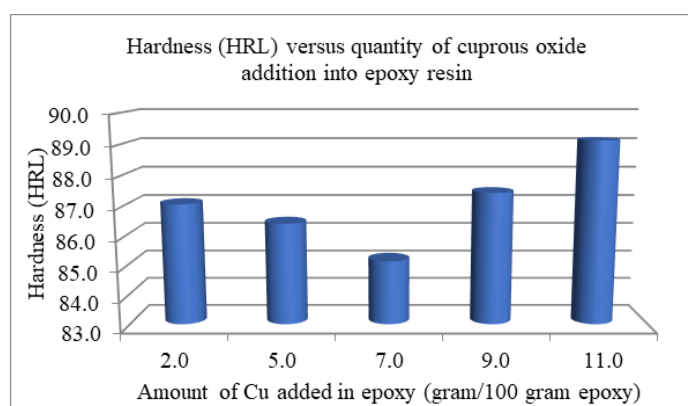


FIGURE 13. Rockwell hardness (HRL) test results

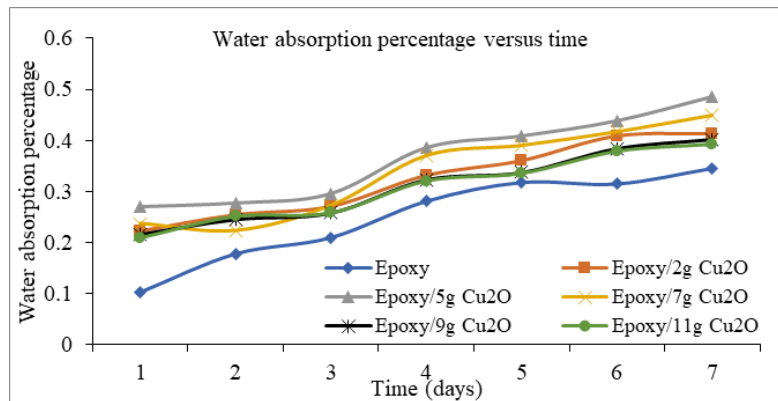


FIGURE 14. Water absorption test results

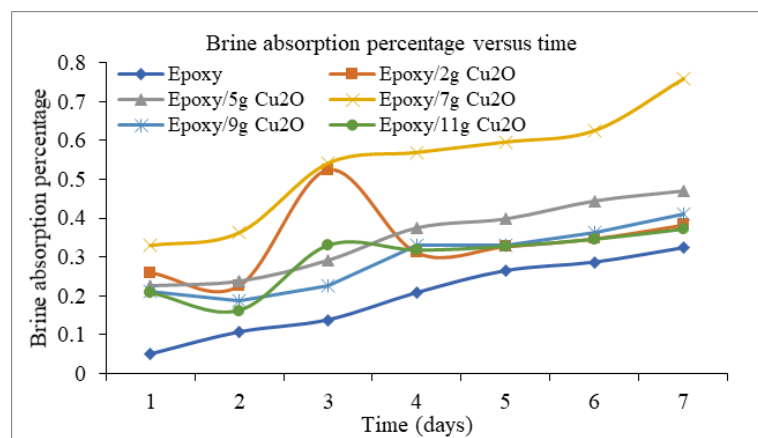


FIGURE 15. Brine absorption test results

TABLE 5. Results of preliminary and post abrasion

Sample	Contact angle (°)	
	Pre abrasion	Post abrasion
Epoxy	67.4 ± 0.07	104.9 ± 0.46
Epoxy/2g Cu2O	94.2 ± 2.11	97.3 ± 8.25

related to the surface of coating. The top of the coating surface had little craters as shown in Figure 10, which may also be a major factor why the contact angle differed for every random spot. Another major factor for the unmodified epoxy to have higher contact angle could be due to the curing of that sample was better than the other coating.

CONCLUSION

Overall, Epoxy/2g Cu<sub>2</sub>O sample was observed to have the highest hydrophobicity, acceptable water and brine absorption, moderate hardness values, and possessed high glass transition temperature, indicating the composite to have good thermal stability. However, cuprous oxide coating quality could be better if the particle size of filler nano sized with small standard deviation in its range of size. As a recommendation, the cuprous oxide powder should be

filtered to have uniform size fillers, and surface modification of the filler should be studied for further improvement of this research.

ACKNOWLEDGEMENT

The authors would like to thank Bina Paint Industries Sdn. Bhd. and Universiti Kebangsaan Malaysia for their technical, financial, and resource and material support. The authors would also like to thank Ministry of Higher Education Malaysia and Universiti Kebangsaan Malaysia for FRGS/1/2018/TK05/UKM/02/4 and GUP-2017-041 grants and laboratory usage.

DECLARATION OF COMPETING INTEREST

None.

REFERENCES

Adeleye, A.S., Oranu E.A., Tao, M. & Keller, A.A. 2016. Release and detection of nanosized copper from a commercial antifouling paint. *Water Research* 102: 374-382.



- Bruice, Y.P. 2014. *Organic Chemistry*. Edisi ketujuh. England: Pearson Education Limited.
- Chambers, L.D., Stokes, K. R., Walsh, F.C. & Wood, R.J.K. 2006. Modern approaches to marine anti-fouling coatings. *Surface and Coatings Technology* 202(2): 412-413.
- Corrosionpedia. 2017. Coating. <https://www.corrosionpedia.com/definition/286/coating-corrosion> [26 Novemver 2017]
- Corrosionpedia. 2017. Marine Coatings. <https://www.corrosionpedia.com/definition/1754/marine-coatings> [26 November 2017]
- Dafforn, K.A., Lewis, J.A. & Johnston, E.L. 2011. Antifouling strategies: History and regulation, ecological impacts and mitigation. *Marine Pollution Bulletin* 3(62): 453-465.
- El Saeed, A. Abd El-Fattah, M. Azzam, A. & Dardir, M.M.B. 2016. Synthesis of cuprous oxide epoxy nanocomposite as an environmentally antimicrobial coating. *International Journal of Biological Macromolecules* (89): 190-197.
- European Chemical Agency. 2012. Understanding Biocidal Products Regulation. <https://echa.europa.eu/regulations/biocidal-products-regulation/understanding-bpr> [25 November 2017]
- Holmes, L.& Turner, A. 2009. Leaching of hydrophobic Cu and Zn from discarded marine antifouling paint residues: Evidence for transchelation of metal pyrithiones. *Environmental Pollution* 157(12): 3440-3444.
- Hou, Y., Hu, W., Gui, Z. & Hu, Y. 2017. Effect of cuprous oxide with different sizes on thermal and combustion behaviors of unsaturated polyester resin. *Journal of Hazardous Materials* 333: 39-48.
- Jagtap, S.D., Tambe S.P., Choudhari, R.N. & Mallik B.P. Mechanical and anticorrosive properties of non toxic coal-tar epoxy alternative coating. *Progress in Organic Coatings* 77(2): 395-402.
- Johnson, T. 2018. Epoxy resin. <https://www.thoughtco.com/what-is-epoxy-resin-820372> [9 April 2018].
- Lambourne, R., & Strivens, T. A. 1999. Paint and surface coatings-Theory and practice” “ 5.18 Ultraviolet absorbers” 195-196
- Mirmohseni, A. & Zavareh, S. 2010. Preparation and characterization of an epoxy nanocomposite toughened by a combination of thermoplastic, layered and particulate nanofillers. *Materials and Design* 31(6): 2699-2706.
- Noor Idora, M.S., Ferry, M., Wan Nik W.B. & Jasnizat, S. 2015. Evaluation of tannin from *Rhizophora apiculata* as natural antifouling agents in epoxy paint for marine application. *Progress in Organic Coatings* 81:125-131.
- Ray, R. & Henshaw, P. 2017. Atomizers and Finish Properties of Surface Coatings. *Comprehensive Materials Finishing* 1(3): 149-157.
- RTI Laboratories. 2015. <http://rtilab.com/techniques/ftir-analysis/> [30 April 2018].
- Science Learning Hub. 2010. Ocean salinity. <https://www.sciencelearn.org.nz/resources/686-ocean-salinity> [30 April 2018].
- Singh, N. & Turner, A., Leaching of copper and zinc from spent antifouling paint particles. *Environmental Pollution* 157(2): 371-376.
- Wallström, E., Jespersen, H. T. & Schaumburg, K. 2011. A new concept for anti-fouling paint for Yachts. *Progress in Organic Coatings* 1(72): 109-114.
- Yebra, D.M., Kiil, S., Weinell C.E. & Johansen, K.D. 2006. Presence and effects of marine microbial biofilms on biocide-based antifouling paints. *Biofouling* 22(1):33-41.
- Yebra, D., & Weinell, C., Key issues in the formulation of marine antifouling paints. *Advances in Marine Antifouling Coatings and Technologies* 17: 308-333.

